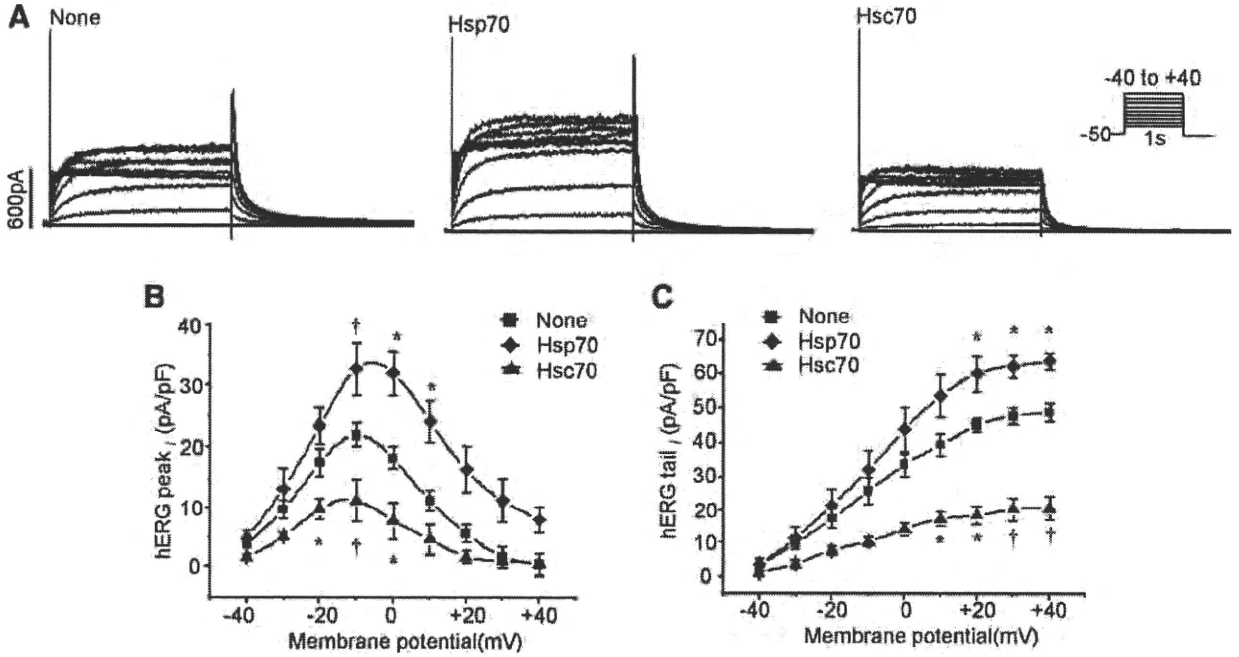

Figure 4. Effects of Hsp70/Hsc70 on hERG currents in HEK293 cells stably expressing hERG-FLAG. Representative current traces recorded from cells transfected with Hsp70 or Hsc70 or mock plasmid (none) **(A)**. The membrane potential was held at −50 mV, depolarized by 1-sec test pulses ranging from −40 to +40mV and then repolarized back to the holding potential for tail current measurement. Average current–voltage relationships of peak and tail currents are shown in **B** and **C**. Values represent means±SEM. Differences between the control and the group with Hsp70 or Hsc70 were tested statistically. *$P<0.05$, †$P<0.01$ vs none (n=17 to 19).

siRNA prolonged half-life of both mutants. However, the effects were more prominent in F805C mutant (76% increase) than in P596R (29% increase) (Figure 8B).

Because HS could decrease the association of Hsc70 with hERG, we examined effects of HS on the stability of WT and 10 kinds of mutant hERG in transfected HL-1 cells. On IBs, WThERG-FLAG gave 2 intense bands, whereas the mutant proteins gave only a faint 135-kDa band (Figure 8C). HS dramatically increased not only the levels of the mature form of WT but also those of mutant hERG, and again this effect of HS was more prominent in those mutant proteins with intracellular domain mutations than those mutant located in the pore-region.

Previous studies have shown that specific hERG mutants can be stabilized by incubating the cells at low temperature.[4] We examined whether expression of hERG and its association with Hsp70 and Hsc70 were affected by hypothermia. WThERG-FLAG, P596R-FLAG, F805C-FLAG, R752W-FLAG and G601S-FLAG were transfected into HEK293 cells, then the cells were cultured at 37°C for 24 hours then at 27°C for 24 hours. The hypothermia increased not only the levels of WT mature and immature forms but also the levels of 2 forms of mutants (Figure 8D). IP experiment showed that the hypothermia decreased the association of mutant hERG with Hsc70 but not with Hsp70, suggesting that both WT and

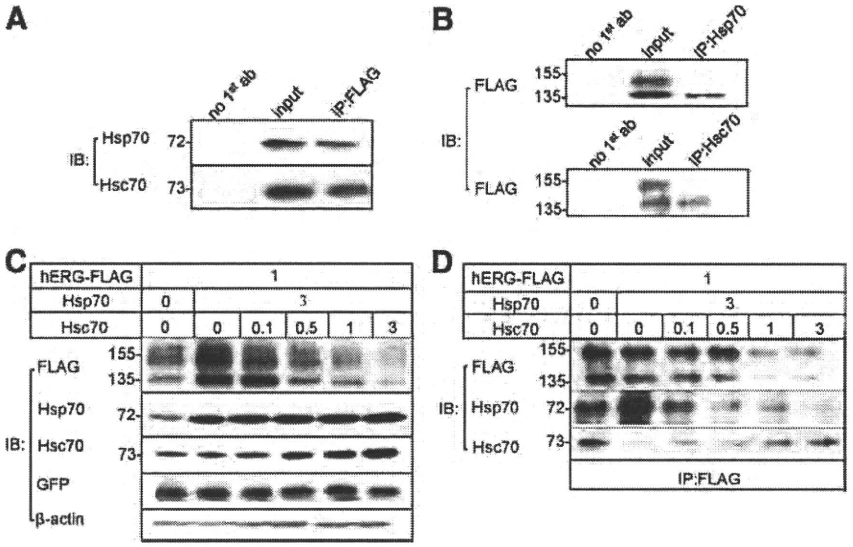

Figure 5. Effects of Hsc70 on Hsp70-induced increase of hERG-FLAG. A, Association of hERG-FLAG with Hsp70 or Hsc70. Anti-FLAG IPs from HEK293 cells transiently expressing hERG-FLAG were subjected to IB with anti-Hsp70 or Hsc70 antibody. No 1st ab represents a negative control with no primary antibody added and input is positive control. **B,** Anti-Hsp70 or Hsc70 IPs from HEK293 cells transiently expressing hERTG-FLAG were subjected to IB with anti-FLAG. **C,** HEK293 cells were transfected with indicated plasmids (μg). Whole-cell lysates were subjected to IB with indicated antibodies (n=4 to 6). **D,** Anti-FLAG IPs were subjected to IB with either anti-FLAG, Hsp70, or Hsc70 (n=6 to 7).

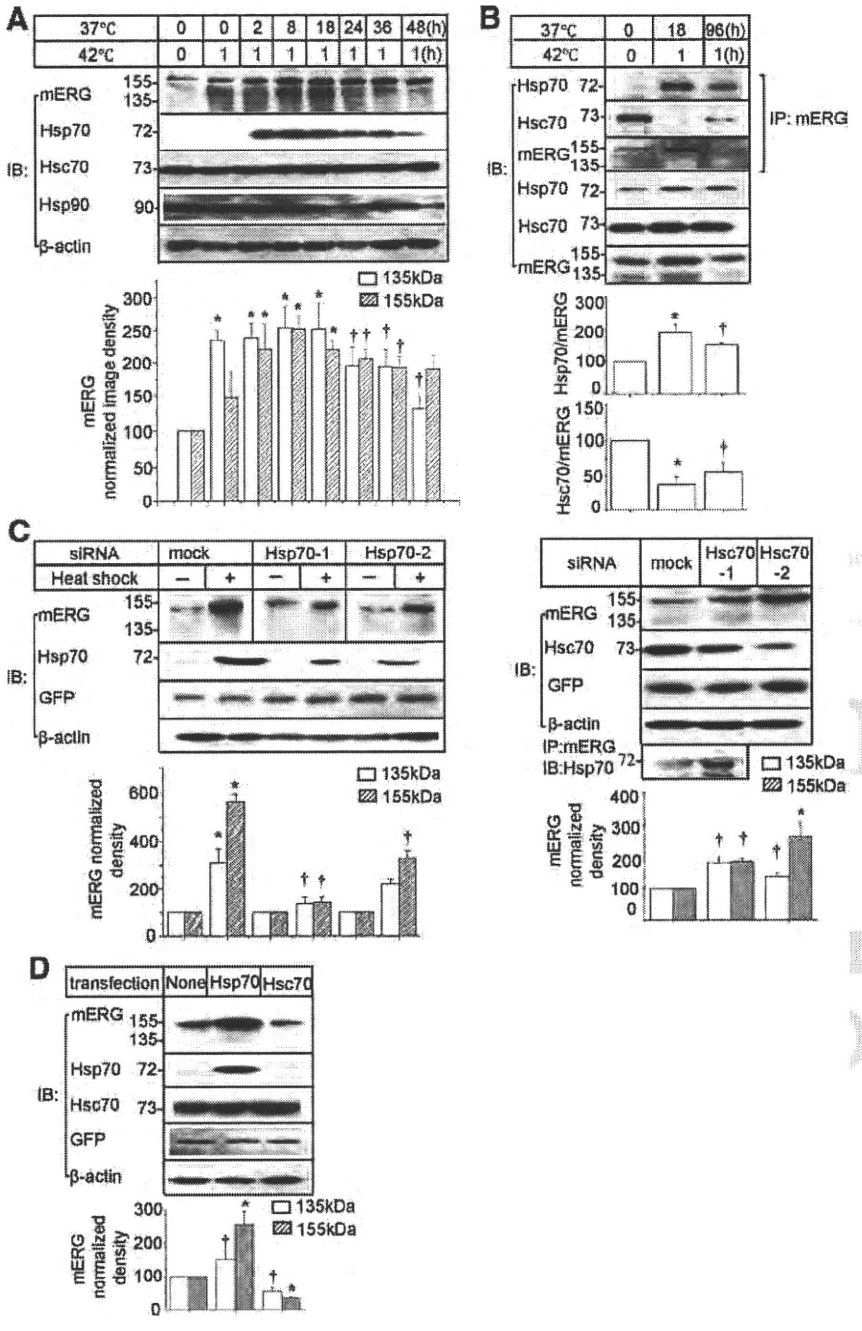

Figure 6. Effects of HS on the level of endogenous mouse ERG (mERG) in HL-1 cells. A, Cells were given a heat shocked at 42°C for 1 hour. The cells were recovered at the indicated times and analyzed by IB with indicated antibodies. Image densities of the immature and mature forms of mERG bands normalized to mERG expression levels in non-HS control cells (n=6 to 7, *$P<0.01$, †$P<0.05$ vs non-HS). **B,** Association of mERG with Hsp70 or Hsc70 was detected by IB. Anti-mERG IPs was subjected to IB. **Bar graphs** show the levels of Hsp70 or Hsc70 associated with mERG (n=4 to 5, *$P<0.01$, †$P<0.05$ vs non-HS group). **C,** HL-1 Cells were transfected with a scramble siRNA (mock) or siRNAs against mouse Hsp70 **(left)** or Hsc70 **(right)**.The levels of mERG, Hsp70, and Hsc70 were analyzed by IB. Image density of mERG were quantified and normalized to mERG levels in the cells with a scramble siRNA (n=5 to 6, *$P<0.01$ vs non-HS; †$P<0.05$ vs with a scramble siRNA with HS). **D,** Effects of Hsp70 or Hsc70 on endogenous mERG. HL-1 cells were transfected either with pcDNA3, Hsp70, or Hsc70 plasmid. Cell lysate was subjected to IB with the indicated antibodies (n=5 to 7, *$P<0.01$; †$P<0.05$ vs none).

mutant hERG proteins were stabilized because of disassociation from Hsc70 at low temperature.

Discussion

In the present study, we found that Hsp70 and Hsc70 exert opposite effects on the stability of hERG, ie, Hsp70 stabilized hERG, whereas Hsc70 destabilized it. The main site of action of these chaperones appeared to be the ER. Both Hsp70 and Hsc70 could associate with hERG and the stability control appeared to be a direct consequence of their association. We have also shown that the levels of these chaperones influenced cardiac APD. Evidence was also presented that disease-causing missense mutations of hERG alter its association with these chaperones.

Hsp70 and Hsc70 Exert Opposite Effects on the Stability of hERG

Hsp70 could be induced by HS and cellular stress, whereas Hsc70 is constitutively expressed.[23] These 2 proteins have a high degree of sequence homology and have been believed to be functionally interchangeable.[24–26] This is the first report to demonstrate that Hsp70 and Hsc70 exert opposite effects on the stability of hERG protein through their association with the immature form. In general, Hsp70 acts on nascent and newly synthesized proteins to hold them in a state competent for proper folding.[11] In contrast, Hsc70 associates with newly synthesized proteins to promote their proteasomal degradation. This effect of Hsc70 has been demonstrated for

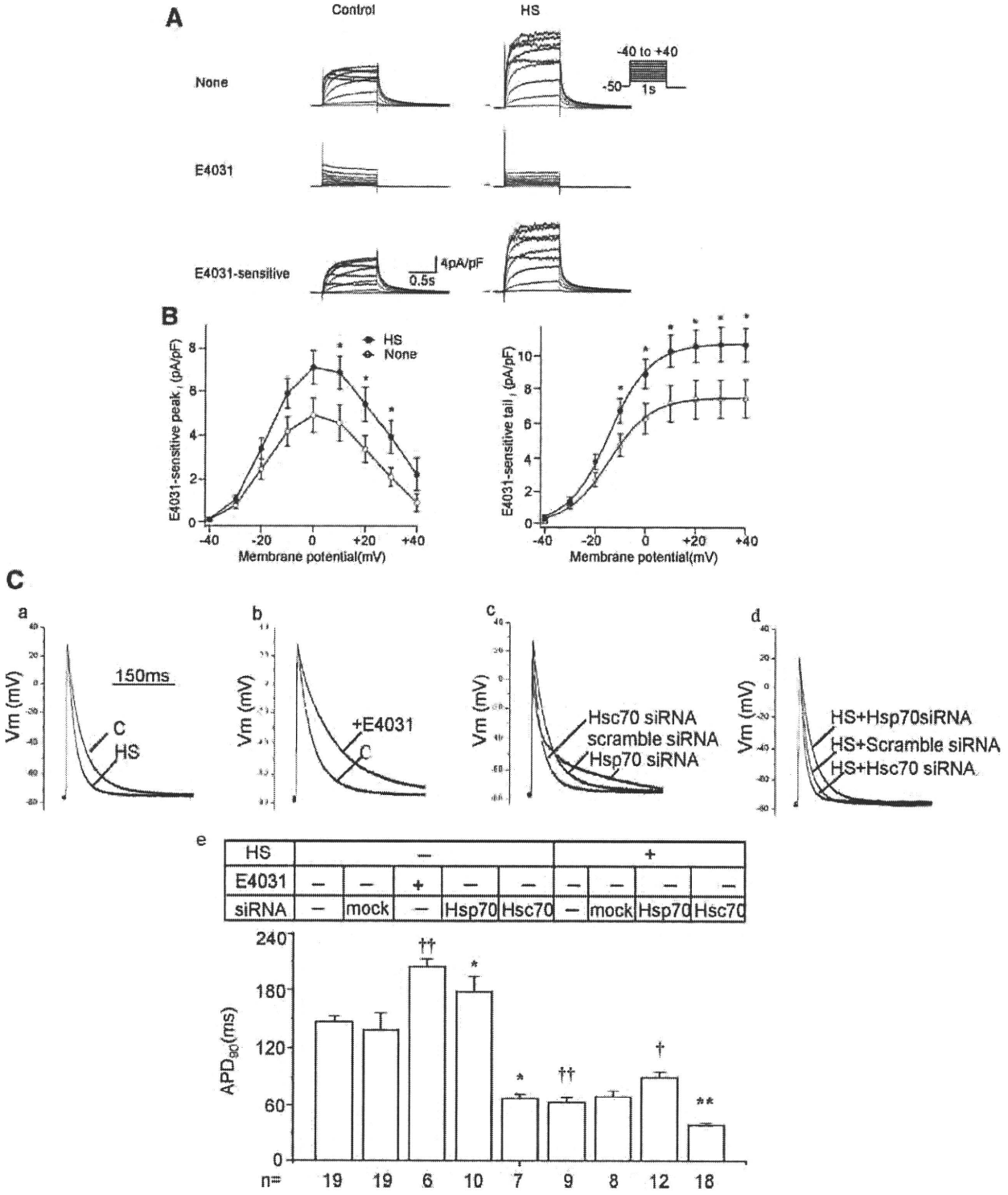

Figure 7. Effects of HS on E4031-sensitive currents and APD. A, Whole-cell membrane currents were recorded from a single HL-1 cell before (none) and after application of 10 μmol/L E4031. E4031-sensitive currents were obtained by digital subtraction. Current recordings were performed 24 hours after HS treatment at 42°C for 1 hour. **B,** Current–voltage relationships of the peak and tail of the E4031-sensitive currents (n=16, *$P<0.05$ vs none). **C,** Action potentials were recorded 24 hours after transfection of a scramble siRNA (mock) or a siRNA against Hsp70 or Hsc70 in the absence or presence of 10 μmol/L E4031. Representative action potentials are shown **(a through d)**. APD_{90} values are summarized as a bar graph **(e)**, and statistically evaluated: ††$P<0.01$ vs non-HS; *$P<0.01$ vs a scramble siRNA control non-HS; †$P<0.05$, **$P<0.01$ vs a scramble siRNA with HS treatment.

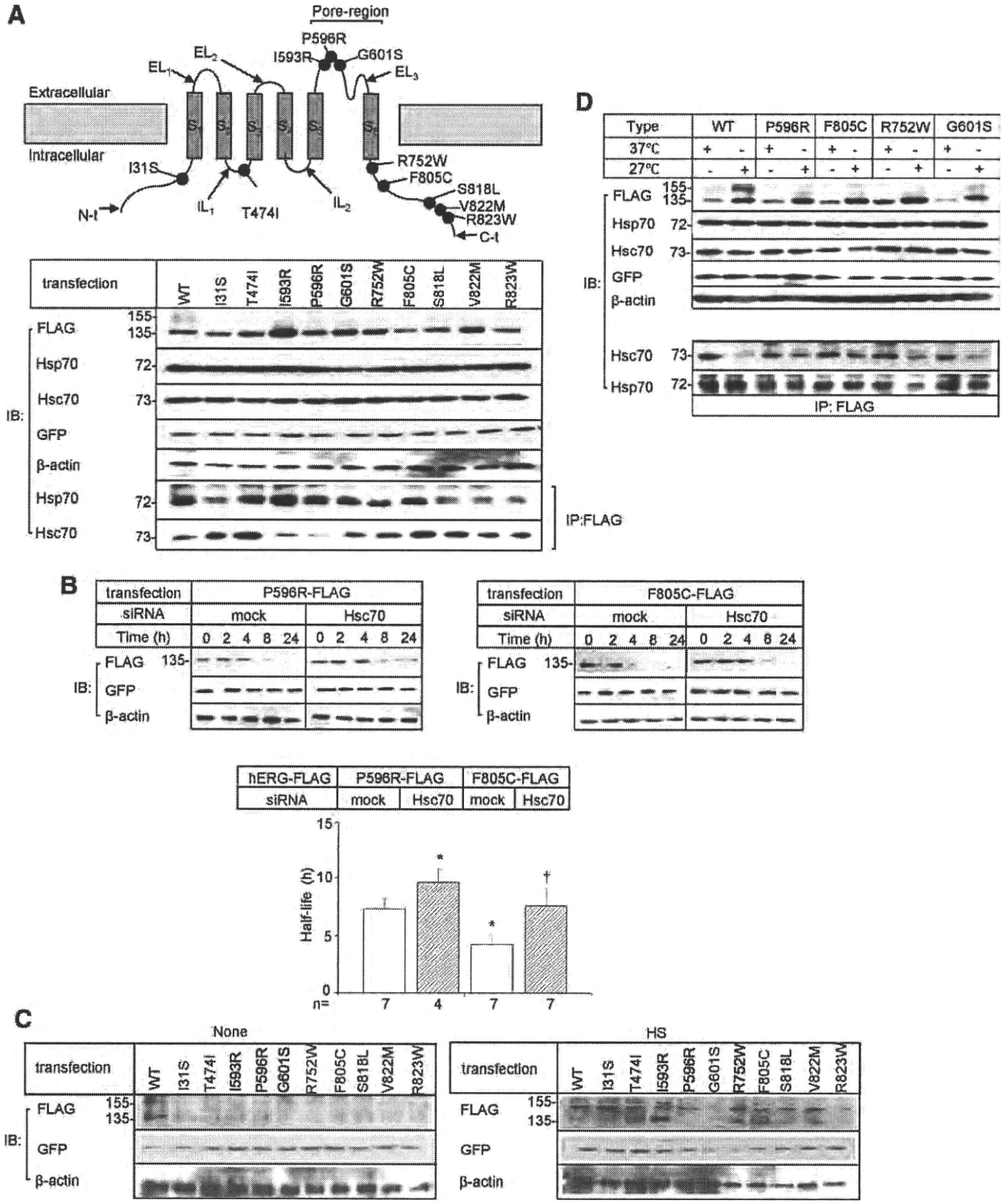

Figure 8. Effects of Hsp70 and Hsc70 on mutant hERG-FLAG. A, Top, Locations of LQT2-associated 10 mutations. **Black circles** indicate the locations of 10 missense mutations. The **arrows** point N terminus (N-t), intracellular loop (IL), extracellular loop (EL), and C terminus (C-t), respectively. WT hERG-FLAG and 10 kinds of mutant hERG-FLAG were transfected into HEK293 cells. Cell lysates or anti-FLAG IPs were subjected to IBs with indicated antibodies **(bottom). B,** Degradation of mutant hERG-FLAG. P596R-FLAG or F805C hERG-FLAG was transfected in HEK293 cells either with a scramble siRNA (mock) or an siRNA against Hsc70. Cells were chased for the indicated times after the addition of cycloheximide. Shown are representative Western blot with the indicated antibodies. Bar graphs summarize the half-life of 2 missense mutant hERG-FLAG. *$P<0.05$ vs P596R-FLAG with a scramble siRNA; †$P<0.05$ vs F805C-FLAG with a scramble siRNA. **C,** WT and mutant hERG-FLAG were transfected into HL-1 cell and the cells were given 1 hour of HS treatment at 42°C. Cell lysates were subjected to IB with indicated antibodies (n=4). **D,** Effects of hypothermia on WT and mutant hERG. Each construct was transfected into HEK293 cells. The cells were cultured at 37°C for 24 hours then at 27°C for 24 hours. The whole-cell lysates or anti-FLAG IPs were analyzed by IB with indicated antibodies (n=5 to 6).

CFTR,[27–29] murine epithelial sodium channel,[13] and $ASIC_2$ (acid-sensing ion channels).[30] Our findings are in agreement with those previous studies and presented evidence that Hsp/Hsc70 association with hERG is regulated by the cellular levels of these 2 chaperones (Figure 5C and 5D).

Hsp70/Hsc70 Controlled the Level of Endogenous mERG and the Cardiac APD

In this study, we identified that E4031-sensitive currents are the predominant component of the outward currents and show essentially the same characteristics as I_{Kr} in HL-1 murine cardiomyocytes. We demonstrated, for the first time, that HS was able to increase I_{Kr} and shorten cardiac APD. Under control conditions, Hsc70 associated with mERG to reduce the cellular level of mERG. HS- induced Hsp70 increases Hsp70-mERG complexes, causing an increase in the cellular level of mERG. The level of mERG is well known to regulate the activity of I_{Kr}[31] and I_{Kr} regulates cardiac APD, especially in mouse atrial myocytes,[19,32] which is one of the major factors to determine the QT interval.[22] E4031-induced prolongation of APD_{90} was more remarkable in the cells treated with HS than in the control cells, indicating that the increased I_{Kr} contributes to acceleration of repolarization by HS through increases in Hsp70-mERG complex associated with decreases of Hsc70-mERG complex. These data strongly suggest that Hsp70/Hsc70 plays a pivotal role in controlling APD in cells treated with HS. Our findings might explain fever-induced shortening of the QT interval.[33,34] Interestingly, siRNA knockdown of Hsc70 shortened APD in HL-1 cells, indicating that Hsc70 is able to regulate APD under physiological conditions. These results are in accordance with antiarrhythmic effects of augmented expression of hERG that have been reported in rabbit ventricular primary culture and a transgenic mice model.[35,36] In both cases, hERG expression resulted in significant shortening of APD and decreased the incidence of early afterdepolarizations.

Stability Control of hERG Mutant Proteins by Hsp70 and Hsc70

Most of LQT2 missense mutations decrease the stability of hERG.[4] This instability has been associated with increased association with Hsp70/ Hsc70, which have been suggested to play similar function.[8] We found that the association of Hsp70 and Hsc70 with mutant channels depended on the nature of the mutation. The level of Hsc70-F805C hERG complexes was higher than that of Hsc70–P596R hERG complexes resulting in a shorter half- life of F805C hERG proteins. The F805C mutant yielded smaller hERG currents than the P596R mutant.[4] Silencing Hsc70 prolonged the half-life of both mutant proteins but more predominantly in F805C, suggesting that Hsc70 determines degradation of their immature forms, especially those with the intracellular mutations.

Accordingly, HS promoted the maturation of mutant hERGs with mutations in intracellular domains rather than those in pore-region. It is conceivable that the HS-induced Hsp70 causes a disassociation of Hsc70 from mutant hERGs and increases the level of Hsp70-hERG complexes. hERG proteins contain a PAS (Per, Arnt, and Sim) domain on their N terminus and a cNBD domain on their C terminus; both of them may be targeted by cytosolic chaperones.[8] LQT2 mutations located in the N or C terminus might interfere the association of chaperones.[5] Ficker E et al reported decreased association of WT and mutant with Hsp70 /Hsc70 and increased hERG with reduced temperature.[8] We detected association of Hsp70 or Hsc70 with hERG separately and found that hypothermia decreased the level of Hsc70 associated with hERG, whereas it unaltered the level of Hsp70. Thus, the degradation of immature form of both WT and mutant hERG proteins was prevented by disassociation of Hsc70 under hypothermia. The biophysical characteristics of mutant hERG may be comparable with CFTRΔ508, a trafficking-deficient mutant. CFTRΔ508 can be rescued by Hsp70 and low-temperature culturing.[37,38] Both HS and low temperature result in disassociation of Hsc70 from mutant hERG proteins and stabilization of the immature form. Our data raise the possibility that Hsc70 and Hsp70 may be a target in the treatment of LQT2 which results from missense hERG mutations.

Acknowledgments

We acknowledge Dr William C. Claycomb (Louisiana State University) for the generous gift of HL-1 cells.

Sources of Funding

This work was supported by Ministry of Education, Culture, Sport, Science and Technology-Japan grant 21590931.

Disclosures

None.

References

1. Sanguinetti MC, Jiang C, Curran ME, Keating MT. A mechanistic link between an inherited and an acquired cardiac arrhythmia: HERG encodes the I_{Kr} potassium channel. *Cell*. 1995;81:299–307.
2. Sanguinetti MC, Tristani-Firouzi M. hERG potassium channels and cardiac arrhythmia. *Nature*. 2006;440:463–469.
3. Kiehn J, Lacerda AE, Wible B, Brown AM. Molecular physiology and pharmacology of HERG. Single-channel currents and block by dofetilide. *Circulation*. 1996;94:2572–2579.
4. Anderson CL, Delisle BP, Anson BD, Kilby JA, Will ML, Tester DJ, Gong Q, Zhou Z, Ackerman MJ, January CT. Most LQT2 mutations reduce Kv11.1 (hERG) current by a class 2 (trafficking-deficient) mechanisms. *Circulation*. 2006;113:365–373.
5. Thomas D, Kiehn J, Katus HA, Karle CA. Defective protein trafficking in hERG-associated hereditary long QT syndrome (LQT2): molecular mechanisms and restoration of intracellular protein processing. *Cardiovasc Res*. 2003;60:235–241.
6. Gong Q, Keeney DR, Molinari M, Zhou Z. Degradation of trafficking-defective long QT syndrome type II mutant channels by the ubiquitin-proteasome pathway. *J Biol Chem*. 2005;280:19419–19425.
7. Gong Q, Anderson CL, January CT, Zhou Z. Role of glycosylation in cell surface expression and stability of HERG potassium channels. *Am J Physiol Heart Circ Physiol*. 2002;283:H77–H84.
8. Ficker E, Dennis AT, Wang L, Brown AM. Role of the cytosolic chaperones Hsp70 and Hsp90 in maturation of the cardiac potassium channel HERG. *Circ Res*. 2003;92:87–100.
9. Petrecca K, Atanasiu R, Akhavan A, Shrier A. N-linked glycosylation sites determine HERG channel surface membrane expression. *J Physiol*. 1999;515:41–48.
10. Jakob U, Gaestel M, Engel K, Buchner J. Small heat shock proteins are molecular chaperones. *J Biol Chem*. 1993;268:1517–1520.
11. Hartl FU, Hayer-Hartl M. Molecular chaperones in the cytosol: from nascent chain to folded protein. *Science*. 2002;295:1852–1858.
12. Walker VE, Atanasiu R, Lam H, Shrier A. Co-chaperone FKBP38 promotes HERG trafficking. *J Biol Chem*. 2007;282:23509–23516.
13. Goldfarb SB, Kashlan OB, Watkins JN, Suaud L, Yan W, Kleyman TR, Rubenstein RC. Differential effects of Hsc70 and Hsp70 on the intracellular trafficking and functional expression of epithelial sodium channels. *Proc Natl Acad Sci U S A*. 2006;103:5817–5822.

14. Kato M, Ogura K, Miake J, Sasaki N, Taniguchi S, Igawa O, Yoshida A, Hoshikawa Y, Murata M, Nanba E, Kurata Y, Kawata Y, Ninomiya H, Morisaki T, Kitakaze M, Hisatome I. Evidence for proteasomal degradation of Kv1.5 channel protein. *Biochem Biophys Res Commun.* 2005;337:343–348.
15. Tanaka H, Miake J, Notsu T, Sonyama K, Sasaki N, Iitsuka K, Kato M, Taniguchi S, Igawa O, Yoshida A, Shigemasa C, Hoshikawa Y, Kurata Y, Kuniyasu A, Nakayama H, Inagaki N, Nanba E, Shiota G, Morisaki T, Ninomiya H, Kitakaze M, Hisatome I. Proteasomal degradation of Kir6.2 channel protein and its inhibition by a Na+ channel blocker aprindine. *Biochem Biophys Res Commun.* 2005;331:1001–1006.
16. Hirota Y, Kurata Y, Kato M, Notsu T, Koshida S, Inoue T, Kawata Y, Miake J, Bahrudin U, Li P, Hoshikawa Y, Yamamoto Y, Igawa O, Shirayoshi Y, Nakai A, Ninomiya H, Higaki K, Hiraoka M, Hisatome I. Functional stabilization of Kv1.5 protein by Hsp70 in mammalian cell lines. *Biochem Biophys Res Commun.* 2008;372:469–474.
17. Koshida S, Kurata Y, Notsu T, Hirota Y, Kuang TY, Li P, Bahrudin U, Harada S, Miake J, Yamamoto Y, Hoshikawa Y, Igawa O, Higaki K, Soma M, Yoshida A, Ninomiya H, Shiota G, Shirayoshi Y, Hisatome I. Stabilizing effects of eicosapentaenoic acid on Kv1.5 channel protein expressed in mammalian cells. *Eur J Pharmacol.* 2009;604:93–102.
18. Claycomb WC, Lanson NA Jr, Stallworth BS, Egeland DB, Delcarpio JB, Bahinski A, Izzo NJ Jr. HL-1 cells: a cardiac muscle cell line that contracts and retains phenotypic characteristics of the adult cardiomyocyte. *Proc Natl Acad Sci U S A.* 1998;95:2979–2984.
19. Toyoda F, Ding WG, Zankov DP, Omatsu-Kanbe M, Isono T, Horie M, Matsuura H. Characterization of the rapidly activating delayed rectifier potassium current, I (Kr), in HL-1 mouse atrial myocytes. *J Membr Biol.* 2010;235:73–87.
20. Xia M, Salata JJ, Figueroa DJ, Lawlor AM, Liang HA, Liu Y, Connolly TM. Functional expression of L- and T-type Ca2+ channels in murine HL-1 cells. *J Mol Cell Cardiol.* 2004;36:111–119.
21. Sartiani L, Bochet P, Cerbai E, Mugelli A, Fischmeister R. Functional expression of the hyperpolarization-activated, non-selective cation current I(f) in immortalized HL-1 cardiomyocytes. *J Physiol.* 2002;545:81–92.
22. Tan HL, Hou CJ, Lauer MR, Sung RJ. Electrophysiologic mechanisms of the long QT interval syndromes and torsade de pointes. *Ann Intern Med.* 1995;122:701–714.
23. Cvoro A, Korac A, Matic G. Intracellular localization of constitutive and inducible heat shock protein 70 in rat liver after in vivo heat stress. *Mol Cell Biochem.* 2004;265:27–35.
24. Takayama S, Xie Z, Reed JC. An evolutionarily conserved family of Hsp70/Hsc70 molecular chaperone regulators. *J Biol Chem.* 1999;274:781–786.
25. Brown CR, Martin RL, Hansen WJ, Beckmann RP, Welch WJ. The constitutive and stress inducible forms of hsp 70 exhibit functional similarities and interact with one another in an ATP-dependent fashion. *J Cell Biol.* 1993;120:1101–1112.
26. Freeman BC, Morimoto RI. The human cytosolic molecular chaperones hsp90, hsp70 (hsc70) and hdj-1 have distinct roles in recognition of a non-native protein and protein refolding. *EMBO J.* 1996;15:2969–2979.
27. Meacham GC, Patterson C, Zhang W, Younger JM, Cyr DM. The Hsc70 co-chaperone CHIP targets immature CFTR for proteasomal degradation. *Nat Cell Biol.* 2001;3:100–105.
28. Zhang H, Peters KW, Sun F, Marino CR, Lang J, Burgoyne RD, Frizzell RA. Cysteine string protein interacts with and modulates the maturation of the cystic fibrosis transmembrane conductance regulator. *J Biol Chem.* 2002;277:28948–28958.
29. Younger JM, Ren HY, Chen L, Fan CY, Fields A, Patterson C, Cyr DM. A foldable CFTR {Delta} F508 biogenic intermediate accumulates upon inhibition of the Hsc70-CHIP E3 ubiquitin ligase. *J Cell Biol.* 2004;167:1075–1085.
30. Vila-Carriles WH, Zhou ZH, Bubien JK, Fuller CM, Benos DJ. Participation of the chaperone Hsc70 in the trafficking and functional expression of ASIC2 in glioma cells. *J Biol Chem.* 2007;282:34381–34391.
31. Guo J, Massaeli H, Xu J, Jia Z, Wigle JT, Mesaeli N, Zhang S. Extracellular K+ concentration controls cell surface density of I_{Kr} in rabbit hearts and of the HERG channel in human cell lines. *J Clin Invest.* 2009;119:2745–2757.
32. Nakamura H, Ding WG, Sanada M, Maeda K, Kawai H, Maegawa H, Matsuura H. Presence and functional role of the rapidly activating delayed rectifier K^+ current in left and right atria of adult mice. *Eur J Pharmacol.* 2010;649:14–22.
33. Karjalainen J, Viitasalo M. Fever and cardiac rhythm. *Arch Intern Med.* 1986;146:1169–1171.
34. Amin AS, Herfst LJ, Delisle BP, Klemens CA, Rook MB, Bezzina CR, underkofler HA, Holzem KM, Ruijter JM, Tan HL, January CT, Wilde AA. Fever-induced QTc prolongation and ventricular arrhythmias in individuals with type 2 congenital long QT syndrome. *J Clin Invest.* 2008;118:2552–2561.
35. Nuss HB, Marban E, Johns DC. Overexpression of a human potassium channel suppresses cardiac hyperexcitability in rabbit ventricular myocytes. *J Clin Invest.* 1999;103:889–896.
36. Royer A, Demolombe S, Harchi AE, Le Quang K, Piron J, Toumaniantz G, Mazurais D, Bellocq C, Lande G, Terrenoire C, Motoike HK, Chevallier JC, Loussouarn G, Clancy CE, Escande D, Charpentier F. Expression of human ERG K^+ channels in the mouse heart exerts anti-arrhythmic activity. *Cardiovasc Res.* 2005;65:128–137.
37. Choo-Kang LR, Zeitlin PL. Induction of HSP70 promotes DeltaF508 CFTR trafficking. *Am J Physiol Lung Cell Mol Physiol.* 2001;281:58–68.
38. Collawn JF, Bebok Z, Matalon. Search and rescue: finding ways to correct deltaF508 CFTR. *Am J Respir Cell Mol Biol.* 2009;40:385–387.

Novelty and Significance

What Is Known?

- The human ether-a-gogo-related gene (hERG) encodes the potassium channel α-subunit, I_{Kr}, and its hereditary dysfunction causes long QT syndrome type 2 (LQT2).
- Heat shock protein (Hsp)70 stabilizes hERG protein to increase I_{Kr}.
- Heat shock cognate (Hsc)70, because of its high degree of sequence homology to Hsp70, may also influence hERG protein.

What New Information Does This Article Contribute?

- We found that Hsc70 destabilizes hERG proteins to decrease I_{Kr}, indicating that Hsc70 and Hsp70 reciprocally control the maturation of hERG proteins. Hsp70 competes with Hsc70 in the binding with hERG and facilitates its maturation.
- Heat shock–induced Hsp70 increases the level of the mature form of missense mutant hERG causing LQT2.

The hERG channel plays an important role in cardiac electric activity. It has been shown that inherited mutations in hERG or pharmacological block of I_{Kr} increases the risk of lethal arrhythmia. Here, we show for the first time that Hsc70 and Hsp70 exert reciprocal effects on stability of hERG proteins. We also found that maturation of disease-causing missense mutant hERGs could be restored by a heat shock. Similar effect was achieved by Hsc70 knockdown through a suppression of Hsc70-degradation pathway. Our study provides a new insight into pathogenesis of inherited arrhythmia at the molecular and cellular levels and may lead to a novel therapeutic approach for treating arrhythmias.

SUPPLEMENTAL MATERIAL

Detailed Methods

Cell culture and transfection

HEK293 cells were cultured in DMEM (Sigma) supplemented with 10% fetal bovine serum (JRH) and penicillin/streptomycin/geneticin at 37°C, 5% CO_2.[14] HL-1 mouse cardiomyocytes were maintained as previously described.[5] An expression construct pcDNA3/hERG-FLAG was engineered by ligating an oligonucleotide encoding a FLAG epitope to the carboxy terminus of hERG cDNA. Missense mutations were introduced into pcDNA3/ hERG-FLAG by site-directed mutagenesis (Figure 8A). pcDNA3 expression plasmid for Hsp70 was provided by A. Nakai and Hsc70 was a gift from Harm H. Kampinga (Groningen, Netherlands). The plasmids were transfected into HEK293 cells using lipofectamine 2000 (invitrongen) following the manufacturer's instructions. The total amount of cDNA was adjusted using vector cDNA. Transfection into HL-1 cells was performed using Nucleofector technology (Amaxa Biosystems, Gaithersburg, MD) following the manufacturer's protocol. For chase experiments, 48h after transfection, cycloheximide (60μg/ml) was added to the culture medium and cells were harvested at indicated time points.

Small interference RNA (siRNA)

Two active oligonucleotides against Hsp70 or Hsc70 and a scrambled control siRNA were used. Table 1 shows sequences of siRNA against Hsp70 and Hsc70. Cells were transfected with siRNA using lipofectamine 2000 (invitrogen) according to manufacturer's instructions.

Immunoblotting and immunoprecipitation

Cells were harvested 48h after transfection and lysed by sonication in a lysis buffer (PBS supplemented with 1% polyoxyethylene (9) octyiphenyl ether (NP-40), 0.5% sodium deoxycholate, 0.1% SDS, 1.5mmol/L aprotinin, 21mmol/L leupeptine, 15mmol/L pepstain and 1 mmol/L phenylmethylsulfonylfluoride). After removal of insoluble materials by centrifugation, protein concentrations were determined with a bicinchoninic acid (BCA) protein assay kit (Pierce, Biotechnology, Rockford, IL). Proteins were separated on SDS-PAGE and electrotransferred to PVDF membranes. The membranes were blocked with 5% non-fat dry milk in PBS plus 0.1% Tween and immunoblotted with a primary antibody. The following antibodies were used: FLAG epitope (Cosmo Bio), Hsp70 (mouse monoclonal; Stressgen), Hsc70 (Rat monoclonal; Stressgen), ubiquitin (Medical & Biological laboratory.Co. Ltd), calnexin (calbiochem), Na^+/K^+ ATPase (upstate), β-actin (Oncogene), GFP (Molecular Probes) and $hKv_{11.1}$ (HERG;Alomone Labs). The blots were developed by using an ECL system (Amersham, Biosciences, Piscataway, NJ). Immunoprecipitation was carried out at 4 °C for overnight in PBS supplemented with 1% Triton X-100, 0.5% SDS, 0.25% sodium deoxycholate, 1 mmol/L EDTA, and protease inhibitors. Immunocomplexes were collected with protein G agarose (Pharmacia, Uppsala, Sweden) and bound proteins were analyzed by SDS-PAGE followed by immunoblotting. Band densities were quantified using a NIH image J software. The all image densities of Western blotting were quantified and normalized to their image densities of ß-actin level.

Optiprep gradient cell fractionation

Cell fractionation was performed as described with a minor modification.[6] 48h after transfection, cells were collected by scraping in a medium (in mmol/L: sucrose 0.25, NaCl 140, EDTA 1, and Tris-HCl 20, pH 8.0) and homogenized by using a polytron. After removal of nuclei by centrifugation, the post-nuclear supernatants were layered onto a 10-40% liner gradient of iodixanolin cell fractionation buffer (Axis-Shild PoC, Oslo, Norway) and centrifuged at 48,000×g at 4℃ for 22h using a Beckman SW41Ti rotor. 22 fractions (0.5 ml each) were collected from the top and were numbered accordingly. Immunoblot analyses were performed using antibodies against organelle markers and hERG-FLAG as indicated.

Immunofluorescence

HEK293 cells were seeded onto gelatin- coated coverslips and transfected with hERG-FLAG, pAcGFP-Golgi or pAcGFP-Mem constructs (Clontech) together with pcDNA3/Hsp70 or Hsc70. 24h after transfection, they were fixed with 4% paraformaldehyde/PBS and then permeabilized with 0.5% Triton X-100. They were incubated for 1h at room temperature with a primary antibody (FLAG, 1:1000; calnexin, 1:200). After blocking in 3% albumin, bound antibodies were visualized with AlexaFluor 546 or 488-conjugated mouse secondary antibody (1:2000), and images were obtained by using a Bio-Rad MRC 1024 confocal microscope. To quantify hERG-FLAG signals, the images of hERG-FLAG signals were cropped with regard to the distribution of each marker proteins (calnexin, Golgi-GFP and GFP1-Mem) using Photoshop CS3 software (Adobe Systems, US). The signal intensities in the cropped images were quantified by Image J software (NIH, US).

Establishment of WThERG-FLAG stable cell line

The plasmids of pcDNA3/hERG-FLAG were transfected into HEK293cells using lipofectamine 2000 following the manufacturer's instructions. The cells were divided 48hours after transfection and cultured at medium containing 1000μg/mL Geneticin (G418). We pick up 60 single clones to culture at the selecting medium for 7 weeks. The expressions of hERG-FLAG were confirmed by Western blot and membrane currents recorded by the whole-cell patch clamp technique showed typical properties of hERG channel currents.

Electrophysiological recordings

HEK293 cells stably expressing hERG-FLAG were transfected with pcDNA3/ Hsc70 or Hsp70 together with pEGFP. The total amount of cDNA was adjusted by vector cDNA. Twenty-four hours after transfection, cells were visualized by EGFP fluorescence and hERG channel currents corresponding to the rapidly-activating delayed-rectifer K^+ channel (I_{Kr}) currents were measured at 37℃ using the whole-cell patch-clamp techniques with an Axopatch-200 amplifier (Axon instrument, USA). Procedures for the current measurement in HL-1 cells were essentially the same as described previously.[7] The extracellular solution contained (mmol/L) : NaCl 140, KCl 4, $CaCl_2$ 1.8, $MgCl_2$ 0.53, NaH_2PO_4 0.33, glucose 5.5, HEPES 5, pH was adjusted to7.4 by NaOH. The internal pipette solution contained (mmol/L) K-aspartate 100, KCl 20, $CaCl_2$ 1, Mg-ATP 5, EGTA 5, HEPES 5, creatine phosphate 5, dipotassium (pH 7.2 with KOH). 0.4μmol/L nisolddipine was included in the bath solution to block $I_{Ca,L}$.[8] The membrane potential was held at -50mV

to inactivate I_{CaT} and avoid I_f activation,[89] depolarized by 1-s test pulses (from -40mV to +40mV in 10mV increments), then repolarized back to the holding potential. Peak amplitudes of the currents during the depolarizing pulses and tail currents during the repolarization were determined and plotted as functions of the potentials of the depolarizing pulses. Action potentials were also measured in the current-clamp mode, elicited at a rate of 0.5 Hz by 5-ms square current pulses of 1nA, and sampled at 20 kHz in the absence or presence of 10 μmol/L E4031 (WAKO, Japan).

Semi-quantitative reverse transcription-PCR (RT-PCR)

Total RNAs were extracted from HEK293 cells using an RNeasy Plus mini kit (QIAGEN) and subjected to RT-PCR assay (Prime Scrips RT-PCR Kit, Takara). RNA samples were treated with DNase I (Promega) to eliminate genomic DNA. Primers used are;

hERG forward primer: CGCTACCACACACAGATGCT, reverse: GATGTCATTCTTCCCCAGGA,

β-actin forward primer: CAACCGTGAAAAGATGAC, reverse: CAGGATCTTCATGAGGTAGT.

PCR products were separated on electrophoresis gel, stained with ethidium bromide, and visualized in a UV transsilluminator.

Statistical analysis

All data are presented as the mean± SEM. For statistical analysis, Student's *t*-test and repeated measures analysis of variance (two-way ANOVA) were used, with $p<0.05$ being considered statistically significant.

Online Figure I

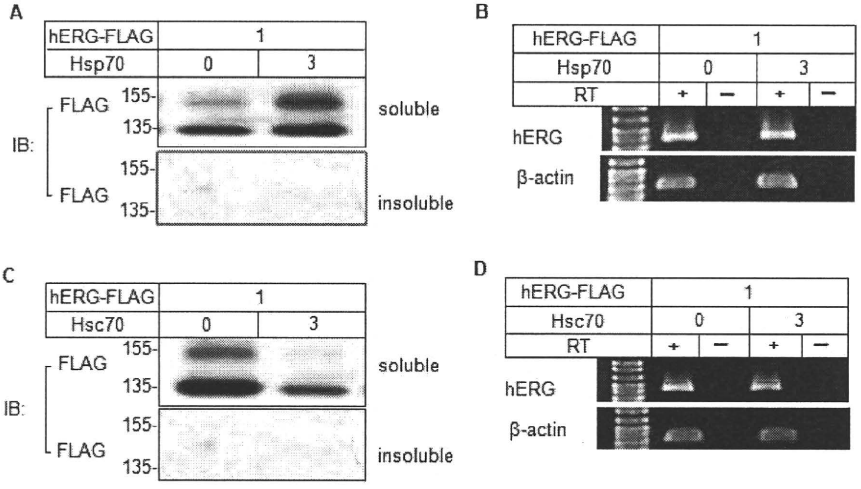

Online Figure I. Effects of Hsp70 or Hsc70 on protein solubility and transcriptional expression of hERG.

HEK293 cells were transiently expressed with hERG-FLAG, GFP and either Hsp70 **(A)** or Hsc70 **(C)** plasmid. The soluble and insoluble fractions of cell lysates were subjected to Western blotting against anti-FLAG antibody.

B and D, Semi-quantitative reverse transcription-PCR (RT-PCR) of hERG mRNA expressed in HEK293 cells (+). β-actin levels were analyzed as control. No band was detected from PCR amplification of RNA without RT (-).

Online Figure II

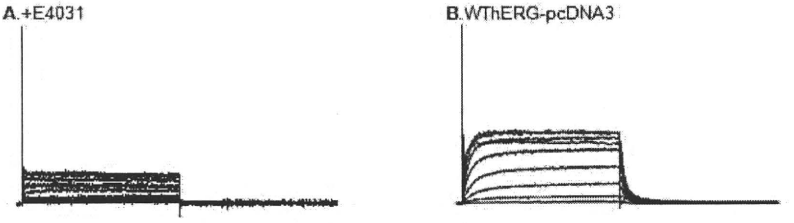

Online Figure II. E4031inhibited hERG currents.

A, A representative trace of whole-cell current mediated by hERG-FLAG in presence of E4031.

B, A representative trace of whole-cell current mediated by hERG-pcDNA3.

Online Figure III

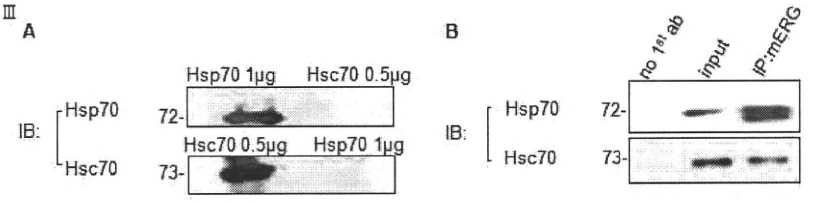

Online Figure III. Bindings of Hsp70 or Hsc70 with endogenous mouse ERG (mERG).

A, Confirmation of the specificity of Hsp70 and Hsc70 antibodies.

Anti-Hsp70 and Hsc70 antibodies were conducted to detect Hsp70 or Hsc70 recombinant proteins by Western blot, respectively.

B, Anti-mERG immunoprecipitates from HL-1 cell lysates were subjected to immunoblotting with anti-Hsp70 or Hsc70 antibody, respectively. Negative control (no 1st ab) and positive control (input) were applied in the first and second lanes.

Online Figure IV

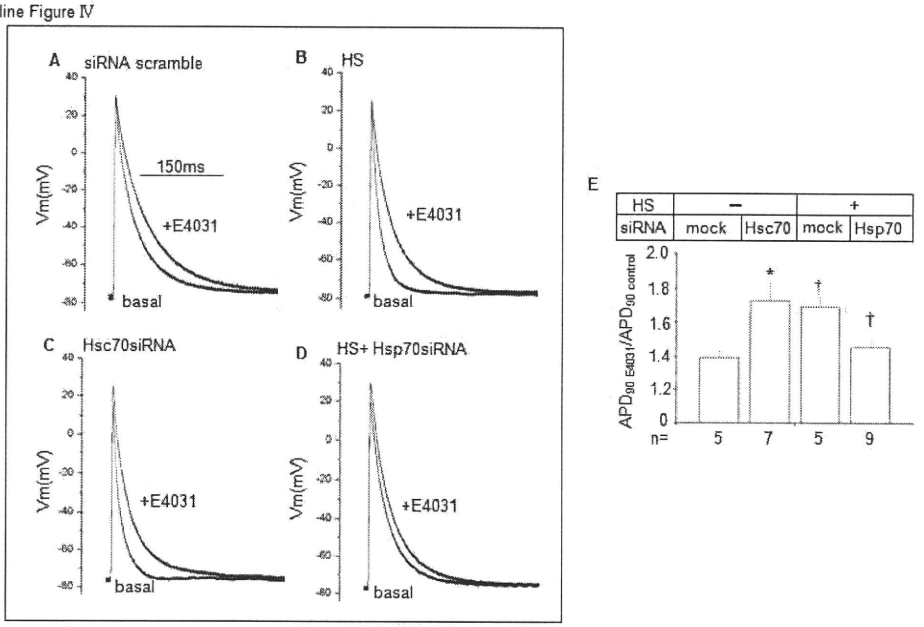

Online Figure IV. The effects of E4031 on APD in HL-1 cells.

Left panel **(A-D)** shows representative action potentials recorded for the indicated groups in the absence or presence of E4031. Bar graphs on the right **(E)** summarize the percentage of APD_{90} prolongation ($APD_{90\ E4031}/APD_{90\ control}$) by E4031 treatment. * $p<0.05$, † $p<0.01$vs a scramble siRNA control with non-HS treatment; † $p<0.05$vs a scramble siRNA control with the HS treatment.

Table Ⅰ, Sequences of siRNA

	sense	antisense
Human Hsp70-2	5'-TCCTGTGTTTGCAATGTTGAATT-3'	5'-UUCAACAUUGCAAACACAGGATT-3'
Human Hsp70-3	5'-TTCAAAGTAAATAAACTTTAATT-3'	5'-UUAAAGUUUAUUUACUUUGAATT-3'
Human Hsc70-2	5'-CCGAACCACUCCAAGCUAUTT-3'	5'-AUAGCUUGGAGUGGUUCGG TT-3'
Human Hsc70-3	5'-CUGUCCUCAUCAAGCGUAATT-3'	5'-UUACGCU UGAUGAGGACAGTT-3'
Mouse Hsp70-1	5'-CUGGAGAUCGACUCUCUGUUC-3'	5'-ACAGAGAGUCGAUCUCCAGGC-3'
Mouse Hsp70-2	5'-CAGUCCGACAUGAAGCACUGG-3'	5'-AGUGCUUCAUGUCGGACUGCA-3
Mouse Hsc70-1	5'-CCGCACCACGCCAAGCUAUGU-3'	5'-AUAGCUUGGCGUGGUGCGGUU-3'
Mouse Hsc70-2	5'-CUAUUGCUUACGGCUUAGAUA-3	5'-UCUAAGCCGUAAGCAAUAGCA-3'

Supplemental References

1. Kato M, Ogura K, Miake J, Sasaki N, Taniguchi S, Igawa O, Yoshida A, Hoshikawa Y, Murata M, Nanba E, Kurata Y, Kawata Y, Ninomiya H, Morisaki T, Kitakaze M, Hisatome I. Evidence for proteasomal degradation of Kv1.5 channel protein. *Biochem. Biophys. Res. Commun.* 2005;337:343-348

2. Tanaka H, Miake J, Notsu T, Sonyama K, Sasaki N, Iitsuka K, Kato M, Taniguchi S, Igawa O, Yoshida A, Shigemasa C, Hoshikawa Y, Kurata Y, Kuniyasu A, Nakayama H, Inagaki N, Nanba E, Shiota G, Morisaki T, Ninomiya H, Kitakaze M, Hisatome I. Proteasomal degradation of Kir6.2 channel protein and its inhibition by a Na+ channel blocker aprindine. *Biochem Biophys Res Commun.* 2005;331:1001-1006.
3. Hirota Y, Kurata Y, Kato M, Notsu T, Koshida S, Inoue T, Kawata Y, Miake J, Bahrudin U, Li P, Hoshikawa Y, Yamamoto Y, Igawa O, Shirayoshi Y, Nakai A, Ninomiya H, Higaki K, Hiraoka M, Hisatome I. Functional stabilization of Kv1.5 protein by Hsp70 in mammalian cell lines. *Biochem Biophys Res Commun.* 2008;372:469-474.
4. Koshida S, Kurata Y, Notsu T, Hirota Y, Kuang TY, Li P, Bahrudin U, Harada S, Miake J, Yamamoto Y, Hoshikawa Y, Igawa O, Higaki K, Soma M, Yoshida A, Ninomiya H, Shiota G, Shirayoshi Y, Hisatome I. Stabilizing effects of eicosapentaenoic acid on Kv1.5 channel protein expressed in mammalian cells. *Eur J Pharmacol.* 2009;604:93-102.
5. Claycomb WC, Lanson NA Jr, Stallworth BS, Egeland DB, Delcarpio JB, Bahinski A, Izzo NJ Jr. HL-1 cells: a cardiac muscle cell line that contracts and retains phenotypic characteristics of the adult cardiomyocyte. *Proc Natl Acad Sci USA.* 1998;95:2979-2984.
6. Woods AJ, Robert MS, Choudhary J, Barry ST, Mazaki Y, Sabe H, Morley SJ, Critchley DR, Norman JC. Paxillin associates with poly (A)-binding protein 1 at the dense endoplasmic reticulum and the leading edge of migrating cells. *J Biol Chem.* 2002;277:6428-6437.
7. Toyota F, Ding WG, Zankov DP, Omatsu-Kanbe M, Isono T, Horie M, Matsuura H. Chearaterization of the rapidly activating delayed rectifier potassium current, I_{Kr}, in Hl-1 mouse atrial myocytes. *J membrane Biol.* 2010;235:73-87.
8. Xia M, Salata JJ, Figueroa DJ, Lawlor AM, Liang HA, Liu Y, Connolly TM. Functional expression of L- and T-type Ca2+ channels in murine HL-1 cells. *J Mol Cell Cardiol.* 2004;36:111-119.
9. Sartiani L, Bochet P, Cerbai E, Mugelli A, Fischmeister R. Functional expression of the hyperpolarization-activated, non-selective cation current I(f) in immortalized HL-1 cardiomyocytes. *J Physiol.* 2002;545:81-92.

EP IMAGE

Remission of Abnormal Conduction and Repolarization in the Right Ventricle After Chemotherapy in Patients With Anterior Mediastinal Tumor

AKASHI MIYAMOTO, M.D., HIDEKI HAYASHI, M.D., PH.D., MAKOTO ITO, M.D., PH.D., and MINORU HORIE, M.D., PH.D.

From the Department of Cardiovascular and Respiratory Medicine, Shiga University of Medical Science, Shiga, Japan

A 22-year-old man with no significant past medical history presented with dry cough that lasted for a couple of months. The patient denied accompanying shortness of breath, palpitation, edema, high fever, or syncope. He had no family history of sudden death. On examination, he was afebrile with a blood pressure of 106/63 mm Hg, pulse rate of 88 beats/min, and normal oxygen saturation. His heart sound was normal without a pericardial rub. ECG (Fig. 1A) displayed a terminal r wave (arrow a) and ST-segment elevation (arrow b) followed by negative deflection of T wave (arrow c) in lead V_1. Chest computed tomography (Fig. 1A) revealed the existence of demarcated tumor in the anterior mediastinal space that attached to the pericardium in front of the right atrium and ventricle. The tumor encompassed the right ventricular outflow tract (arrow) but did not show invasion into the intrapericardial space. The tumor was histologically diagnosed with the large B cell lymphoma from a specimen obtained by needle biopsy. He started to undergo chemotherapy including cyclophosphamide, vincristine, doxorubicin, rituximab, and prednisolone. Two months after the chemotheraphy, chest computed tomography confirmed that the lymphoma size was reduced, which was almost invisible (Fig. 1B). At that time, ECG showed the disappearance of a late r′ wave and ST-segment elevation in lead V_1 (Fig. 1B). These findings indicate that coinciding with the shrinkage of anterior mediastinal tumor, conduction disturbance, and abnormal repolarization in the right ventricle were resolved. No life-threatening arrhythmic event occurred during the follow-up.

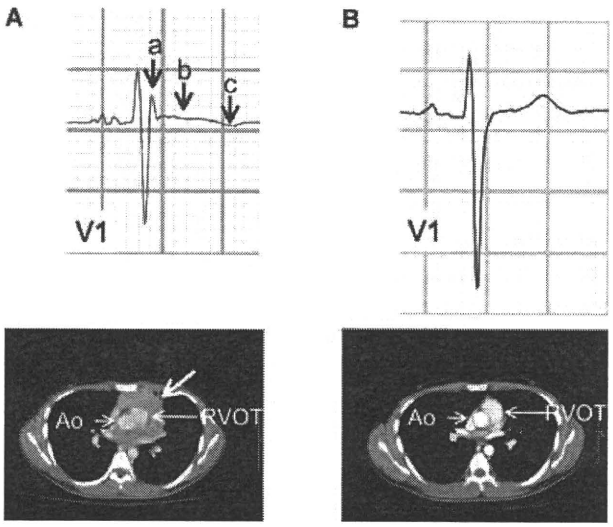

Figure 1. *A and B: ECG recording in lead V_1 and contrast-enhanced computed tomography scan before and after chemotherapy, respectively. Ao = Aorta; RVOT = right ventricular outflow tract.*

J Cardiovasc Electrophysiol, Vol. pp. 1-1.

No disclosures.

Address for correspondence: Hideki Hayashi, M.D., Ph.D., Department of Cardiovascular and Respiratory Medicine, Shiga University of Medical Science, Otsu, Shiga 520-2192, Japan. Fax: 81-77-543-5839; E-mail: hayashih@belle.shiga-med.ac.jp

doi: 10.1111/j.1540-8167.2010.01898.x

Long QT syndrome with compound mutations is associated with a more severe phenotype: A Japanese multicenter study

Hideki Itoh, MD, PhD,* Wataru Shimizu, MD, PhD,† Kenshi Hayashi, MD, PhD,‡ Kenichiro Yamagata, MD,† Tomoko Sakaguchi, MD, PhD,* Seiko Ohno, MD, PhD,§ Takeru Makiyama, MD, PhD,§ Masaharu Akao, MD, PhD,§ Tomohiko Ai, MD, PhD,¶ Takashi Noda, MD, PhD,† Aya Miyazaki, MD,‖ Yoshihiro Miyamoto, MD, PhD,** Masakazu Yamagishi, MD, PhD,‡ Shiro Kamakura, MD, PhD,† Minoru Horie, MD, PhD*

*From the *Department of Cardiovascular and Respiratory Medicine, Shiga University of Medical Science, Otsu, Japan, †Division of Arrhythmia and Electrophysiology, Department of Cardiovascular Medicine, National Cerebral and Cardiovascular Center, Suita, Japan, ‡Division of Cardiovascular Medicine, Kanazawa University Graduate School of Medical Science, Kanazawa, Japan, §Department of Cardiovascular Medicine, Kyoto University Graduate School of Medicine, Kyoto, Japan, ¶Texas Heart Institute/St. Luke's Episcopal Hospital, Houston, Texas, ‖Department of Pediatric Cardiology, National Cerebral and Cardiovascular Center, Suita, Japan, and **Laboratory of Molecular Genetics, National Cerebral and Cardiovascular Center, Suita, Japan.*

BACKGROUND: Long QT syndrome (LQTS) can be caused by mutations in the cardiac ion channels. Compound mutations occur at a frequency of 4% to 11% among genotyped LQTS cases.

OBJECTIVE: The purpose of this study was to determine the clinical characteristics and manner of onset of cardiac events in Japanese patients with LQTS and compound mutations.

METHODS: Six hundred three genotyped LQTS patients (310 probands and 293 family members) were divided into two groups: those with a single mutation (n = 568) and those with two mutations (n = 35). Clinical phenotypes were compared between the two groups.

RESULTS: Of 310 genotyped probands, 26 (8.4%) had two mutations in the same or different LQTS-related genes (compound mutations). Among the 603 LQTS patients, compound mutation carriers had significantly longer QTc interval (510 ± 56 ms vs 478 ± 53 ms, $P = .001$) and younger age at onset of cardiac events (10 ± 8 years vs 18 ± 16 years, $P = .043$) than did single mutation carriers. The incidence rate of cardiac events before age 40 years and use of beta-blocker therapy among compound mutation carriers also were different than in single mutation carriers. Subgroup analysis showed more cardiac events in LQTS type 1 (LQT1) and type 2 (LQT2) compound mutations compared to single LQT1 and LQT2 mutations.

CONCLUSION: Compound mutation carriers are associated with a more severe phenotype than single mutation carriers.

KEYWORDS Compound; Gene; Long QT syndrome; Mutation

ABBREVIATION QTS = long QT syndrome

(Heart Rhythm 2010;7:1411–1418)

Introduction

Congenital long QT syndrome (LQTS) is a heterogeneous disease characterized by prolonged ventricular repolarization and episodes of syncope and/or life-threatening cardiac arrhythmias, particularly polymorphic ventricular tachycardia.[1] Several disease-causing genes have been identified, including genes encoding cardiac ion channel-composing proteins, namely, *KCNQ1* (LQT1), *KCNH2* (LQT2), *SCN5A* (LQT3), *KCNE1* (LQT5), *KCNE2* (LQT6), *KCNJ2* (LQT7), and *CACNA1C* (LQT8), and genes encoding a family of versatile membrane adapters, namely, *ANK2* (LQT4), *CAV3* (LQT9), *SCN4B* (LQT10), *AKAPs* (LQT11), and *SNTA1* (LQT12).[2–5] Two modes of inheritance are involved in this syndrome, which exhibits both an autosomal dominant and an autosomal recessive pattern. The majority of LQTS cases are inherited in an autosomal dominant fashion. This pattern, which has been named as Romano-Ward syndrome,[6,7] can result from a single mutation in one

Drs. Shimizu, Makiyama, Akao, Miyazaki, Miyamoto, Yamagishi, and Horie were supported in part by a Health Sciences Research Grant (H18-Research on Human Genome-002) and a Research Grant for the Cardiovascular Diseases (21C-8) from the Ministry of Health, Labour and Welfare, Japan. Dr. Itoh was supported in part by a Grant-in-Aid for Young Scientists from the Ministry of Education, Culture and Technology. Dr. Horie was supported by the Uehara Memorial Foundation. Drs. Itoh and Shimizu contributed equally to this study. **Address reprint requests and correspondence:** Dr. Wataru Shimizu, Division of Arrhythmia and Electrophysiology, Department of Cardiovascular Medicine, National Cerebral and Cardiovascular Center, 5-7-1 Fujishiro-dai, Suita, Osaka 565-8565, Japan. E-mail address: wshimizu@hsp.ncvc.go.jp. (Received 7 February 2010; accepted June 3, 2010.)

1547-5271/$ -see front matter doi:10.1016/j.hrthm.2010.06.013

of the LQTS candidate genes. On the other hand, Jervell and Lange-Nielsen syndrome, which is inherited in an autosomal recessive fashion, is very rare,[8] affecting less than 1% of LQTS cases. It is caused by homozygous or compound heterozygous mutations of *KCNQ1* or *KCNE1*.[9,10]

Genetic analysis sometimes reveals two or more mutations in LQTS patients with clinical phenotypes of Romano-Ward syndrome. These compound mutations were shown to be associated with an increased arrhythmic risk.[11,12] However, most previous studies were conducted in Caucasian patients, and few systematic studies have involved Asian cohorts. In the present study, we analyzed the clinical characteristics of LQTS patients who were registered in a Japanese multicenter study. Analysis of the more 600 genotyped patients revealed that LQTS patients with compound mutations not only were common in Japan (8.4% among probands) but were associated with longer QTc and earlier onset of cardiac events. In patients who initially are diagnosed as LQT1 or LQT2, additional mutations may be present if patients have a more severe phenotype than expected; therefore, conducting a survey for major LQTS-related genes is critically important.

Methods

Patients and data collection

Major candidate genes were analyzed in 612 consecutive and unrelated probands with a suspected clinical diagnosis of congenital LQTS, who were referred to four centers in Japan (Shiga University of Medical Science, Otsu; Kyoto University Graduate School of Medicine, Kyoto; Kanazawa University Graduate School of Medical Science, Kanazawa; and National Cardiovascular Center, Suita) between June 1996 and January 2009. If gene mutations in LQTS-related genes were identified, further genetic analysis was conducted among family members as extensively as possible. All patients in the cohort were Japanese.

Genetic analysis

Informed consent was obtained from all individuals or their guardians according to standards established by the local institutional review boards. Genotypic and DNA sequence analyses of *KCNQ1, KCNH2, SCN5A, KCNE1,* and *KCNE2* were performed as described previously.[13] In addition, *KCNJ2* (Andersen syndrome [LQT7][14,15]) was analyzed in patients who had not only QT prolongation but also the clinical phenotype of Andersen syndrome, for example, periodic paralysis or dysmorphic features. Other candidate genes (e.g., ankyrin-B [LQT4], *CACNA1C* [Timothy syndrome, LQT8]) were not analyzed because mutations in these genes are extremely rare. Denaturing high-performance liquid chromatography was performed as described previously.[16] Abnormal conformers were amplified by polymerase chain reaction and sequenced using an ABI PRISM310 DNA sequencer (Perkin-Elmer Applied Biosystems, Wellesley, MA, USA). "Splicing error" mutations were defined as those that occurred within three bases of the splicing sites. When mutations were detected, 200 Japanese control subjects were checked and single nucleotide polymorphisms were excluded from the study. If mutations of these genes were detected in the probands, their family members were also analyzed and genotype–phenotype correlations confirmed. Mutation-negative controls were defined as family members without mutations detected in each proband. Nonsynonymous as well as synonymous single nucleotide polymorphisms were excluded with the assistance of data from previous reports[17–19] and from the National Center for Biotechnology Information database.

Clinical characterization

Baseline clinical data were recorded for each patient and included the following: age at diagnosis, age at first cardiac event, sex, cardiac events, family history of sudden cardiac death or LQTS members, ECG measurements, and therapeutic regimens administered. Schwartz scores also were calculated.[20,21] In the analysis of triggers of arrhythmic events, triggers were divided into four categories: exercise/swimming, emotional stress/arousal stress, sleep/rest, and other conditions.

ECG parameters measured at baseline included RR, QT_{end}, QT_{peak}, and $T_{peak\text{-}end}$ ($QT_{end\text{-}peak}$) intervals. The latter is thought to reflect transmural dispersion of ventricular repolarization.[22] Measurements were the mean of at least three beats measured in lead V_5 from the 12-lead ECG during stable sinus rhythm and corrected by the Bazett formula.[23] QT_{end} was manually measured as the time interval between QRS onset (Q) and the point at which the isoelectric line intersected a tangential line drawn at the maximal downslope of the positive T wave or the maximal

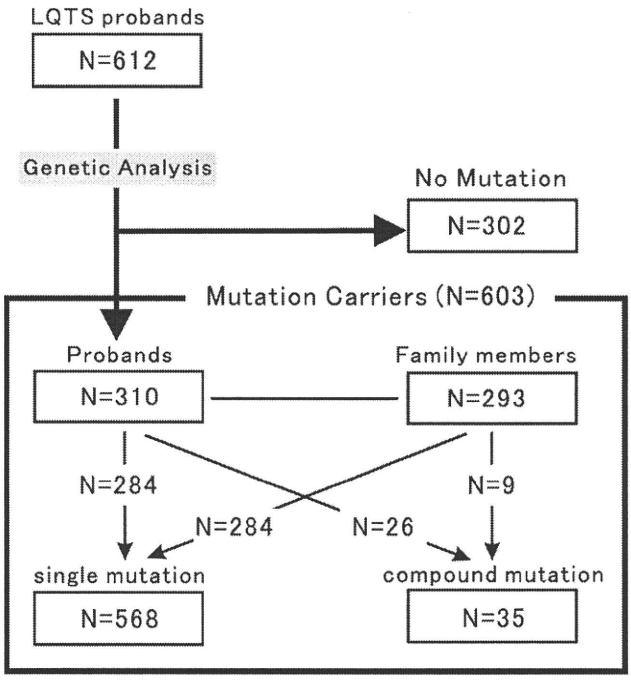

Figure 1 Schematic representation of the positive-mutation carriers in this study. LQTS = long QT syndrome.

Table 1 Overall data of patients with compound mutations

Research groups	Schwartz et al.	Westenkow et al.	Tester et al.	This study
Reported years	2003	2004	2005	2010
The corresponding number in the reference list	25	11	12	
Percentage of probands with compound mutations (probands with compound mutations/total probands) subtypes	4.6% (6/130)	5.2% (9/172*)	10.8% (29/269)	8.4% (26/310)
LQT1	7 (58%)	14 (35%)	30 (52%)	18 (35%)
LQT2	2 (17%)	10 (25%)	15 (26%)	17 (33%)
LQT3	3 (25%)	2 (5%)	13 (22%)	14 (27%)
LQT5-D85N	0 (0%)	10 (25%)	0 (0%)	0 (0%)
vs. single mutation carriers				
QTc interval	NA	prolonged	not significant	prolonged
Cardiac events	NA	frequent	not significant	not significant
Age of onset	NA	NA	younger onset	younger onset

*This table excluded probands with single nucleotide polymorphisms (SNP), NA = not available.

upslope of the negative T wave (QT_{end}). $QT_{end-peak}$ then was obtained by calculating as QT_{end} minus QT_{peak}.

Statistical analysis

All analyses were performed using the SPSS 16.0 statistical package (SPSS, Inc., Chicago, IL. USA). Data are expressed as mean ± SD. $P < 0.05$ was considered significant. Univariate comparison of parameters between groups was performed by an unpaired t-test. Differences in incidence between groups were analyzed by Chi-square test or Fisher exact probability test. The cumulative probability of a first cardiac event (syncope, torsades de pointes, ventricular fibrillation, cardiac arrest, or sudden death) occurring before age 40 years and before beta-blocker therapy or after beta-blocker therapy was determined by means of the life-table method of Kaplan-Meier, and results were compared using log rank test.[24]

Results

Genetic characteristics of mutations associated with single and compound mutations

Genetic analysis revealed gene mutations in 310 (51%) of 612 probands. The study enrolled 603 genotyped LQTS patients consisting of 310 genotyped probands and their 293 genotyped family members. A flowchart of the genetic diagnosis of the study population is shown in Figure 1.

Of the 310 genotyped probands, 26 (8.4%) had compound mutations. This rate is comparable to the rates in previous reports of Caucasian patients (Table 1). The 26 probands all had two mutations in the LQTS-related genes we examined. These 52 mutations in 26 probands consisted of 45 missense mutations, 4 frameshift mutations, 2 splice-site mutations, and 1 nonsense mutation (see Online Supplemental Data 1). The mutation types of the 284 single mutation carriers were 210 missense mutations, 34 frameshift mutations, 18 splicesite mutations, 12 deletions, 9 nonsense mutations, and 1 insertion mutation (see Online Supplemental Data 2). Therefore, the mutation types were similar between the two groups (Figure 2).

Among the 293 genotyped family members, there were 284 single mutation carriers and 9 compound mutation carriers. In total, 568 patients with a single mutation (284 probands and 284 family members) consisted of 256 with LQT1, 248 with LQT2, 62 with LQT3, and 2 with LQT5. Thirty-five compound mutation carriers (26 probands and 9 family members) consisted of 9 with LQT2 and LQT3, 7 with LQT1 and LQT2, 6 with LQT1 and LQT3, 4 with double LQT1, 3 with double LQT2 mutations, 2 with LQT1 and LQT7, 2 with LQT2 and LQT7, 1 with double LQT3, and 1 with LQT1 and LQT6.

Families associated with compound mutations

In the analysis of family members associated with compound mutations, 28 single heterozygous mutation carriers and 4 obligate single mutation carriers were identified from 9 families, and single mutation carriers had milder clinical phenotypes than compound mutation carriers (Figure 3). Only 2 (6%) of the 32 single mutation carriers had syncope but no torsades de pointes, an incidence lower than that in compound mutation carriers (54% [19/35] patients, $P < .001$). For single heterozygous mutation carriers in compound mutation families, average QTc interval was 442 ± 30 ms, which was longer than that of the 15 mutation-negative controls (408 ± 28 ms, $P = .001$) but significantly shorter than that of compound mutation carriers (510 ± 56 ms, $P < .001$).

Early onset of cardiac events and more severe QT prolongation was observed in patients with compound mutations

Table 2 compares the clinical characteristics of 35 LQTS patients with compound mutation and 568 LQTS patients with a single mutation. The female-to-male ratio was similar between the two groups. However, the incidence of family members associated with double-hit patients was significantly smaller than that with a single mutation (26% vs 50%, $P = .005$). In the ECG analysis of 496 patients with available information, corrected QT interval was significantly longer in compound mutation carriers than in single mutation carriers (510 ± 56 ms vs 478 ± 53 ms, respectively, $P = .001$), whereas other ECG findings, R-R interval, corrected QT_{peak}, corrected $QT_{peak-end}$, and rates of

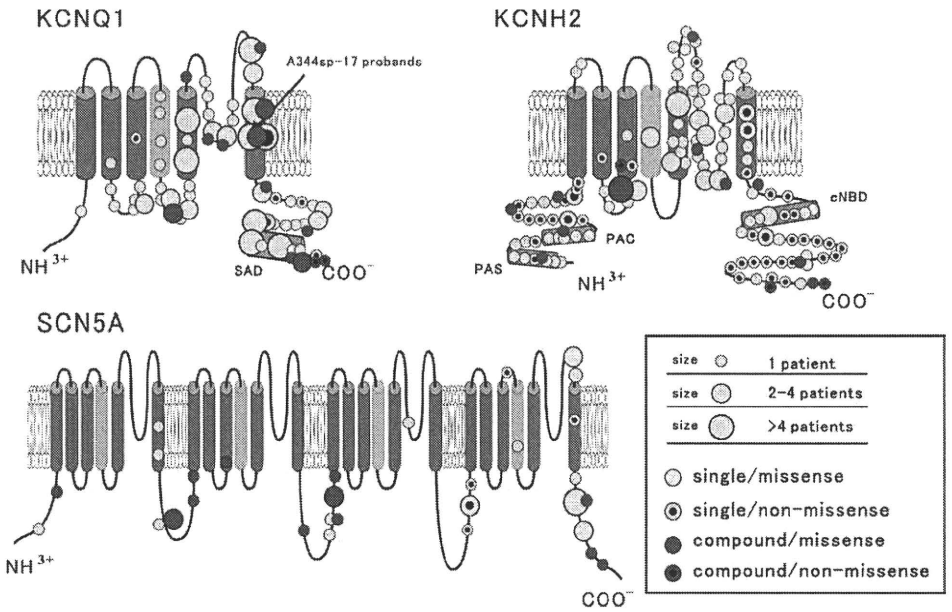

Figure 2 Conventional transmembrane topology of all mutations in the probands.

notched T wave and T-wave alternans were not different between the two groups. The frequency of patients with a normal QTc interval <440 ms was similar between the two groups, whereas the frequency of double-hit patients with QTc intervals >500 ms was significantly higher than in those with a single mutation (66% vs 26%, P <.001). Schwartz scores in the compound mutation group and the rate of patients with a score ≥4 were higher than those in the single mutation group (Schwartz score: 4.3 ± 2.1 vs 3.4 ± 1.9 points, P = .017; rates of Schwartz score ≥4 points: 70% vs 47%, P = .026). A significantly higher number of patients with compound mutations received beta-blocker therapy than did those with a single mutation (56% vs 33%, P = .006).

In the analysis of "all age groups," the frequency of cardiac events was similar between compound and single mutation groups, whereas age at first cardiac event was significantly lower in the compound mutation group (10 ± 8 years vs 18 ± 16 years, P = .043). For the occurrence of syncope or torsades de pointes before age 40 years, compound mutation carriers had significantly more events than did single mutation carriers (54% vs 37%, P = .043). The occurrence of cardiac arrest or ventricular fibrillation was similar between the two groups for patients before age 40 years. In 561 patients with available information on age at first cardiac events, Kaplan-Meier analysis showed that the cumulative rate of survival without a cardiac event before age 40 years and use of beta-blocker therapy differed significantly between compound and single mutation carriers (P = .004 by log rank test; Figure 4A) and between compound mutation carriers and each subgroup of single mutation carriers (P = .004 vs LQT1, P = .018 vs LQT2, P = .001 vs LQT3, by log rank test; Figure 4B). In the analysis of matched subtypes between single and compound mutation carriers, patients with additional mutations in an LQTS subtype had a significantly poorer prognosis than LQT1 alone (P = .001; Figure 5) and LQT2 alone (P = .035) but not LQT3 alone (P = .06).

Discussion

In this multicenter study, the major findings were as follows. (1) LQTS-associated compound mutations in the Japanese population were as common as previously reported in studies of Caucasian patient cohorts. (2) Patients with compound mutations displayed longer QTc and earlier onset of cardiac events. (3) Patients with compound mutations had more cardiac events before age 40 years and more beta-blocker therapy. (4) Subgroup analysis showed more cardiac events in LQT1 and LQT2 compound mutations compared to single LQT1 and LQT2 mutations.

Twenty-six probands (8.4% of genotyped LQTS) were found to have two variants in genes encoding ion channels *(KCNQ1, KCNH2, SCN5A, KCNE1, KCNE2,* or *KCNJ2)*. This incidence rate is in general agreement with other studies that reported a prevalence of compound or multiple mutations of 5% to 11% of genotyped LQTS (Table 1).[11,18,25]

Table 1 summarizes the genetic and clinical characteristics of patients enrolled in previous studies and compares them with the characteristics of patients enrolled in the present study. Sanguinetti and colleagues reported that patients with compound mutations not only had longer QT intervals than single mutation carriers but also had more frequent cardiac events.[11] However, Ackerman and colleagues demonstrated that, although compound mutation carriers were diagnosed at a younger age than single mutation carriers, they did not have significantly longer QT intervals.[12] The difference between these results might be explained by half of the 20 compound probands in the cohort of Sanguinetti et al possessing the common *KCNE1-*

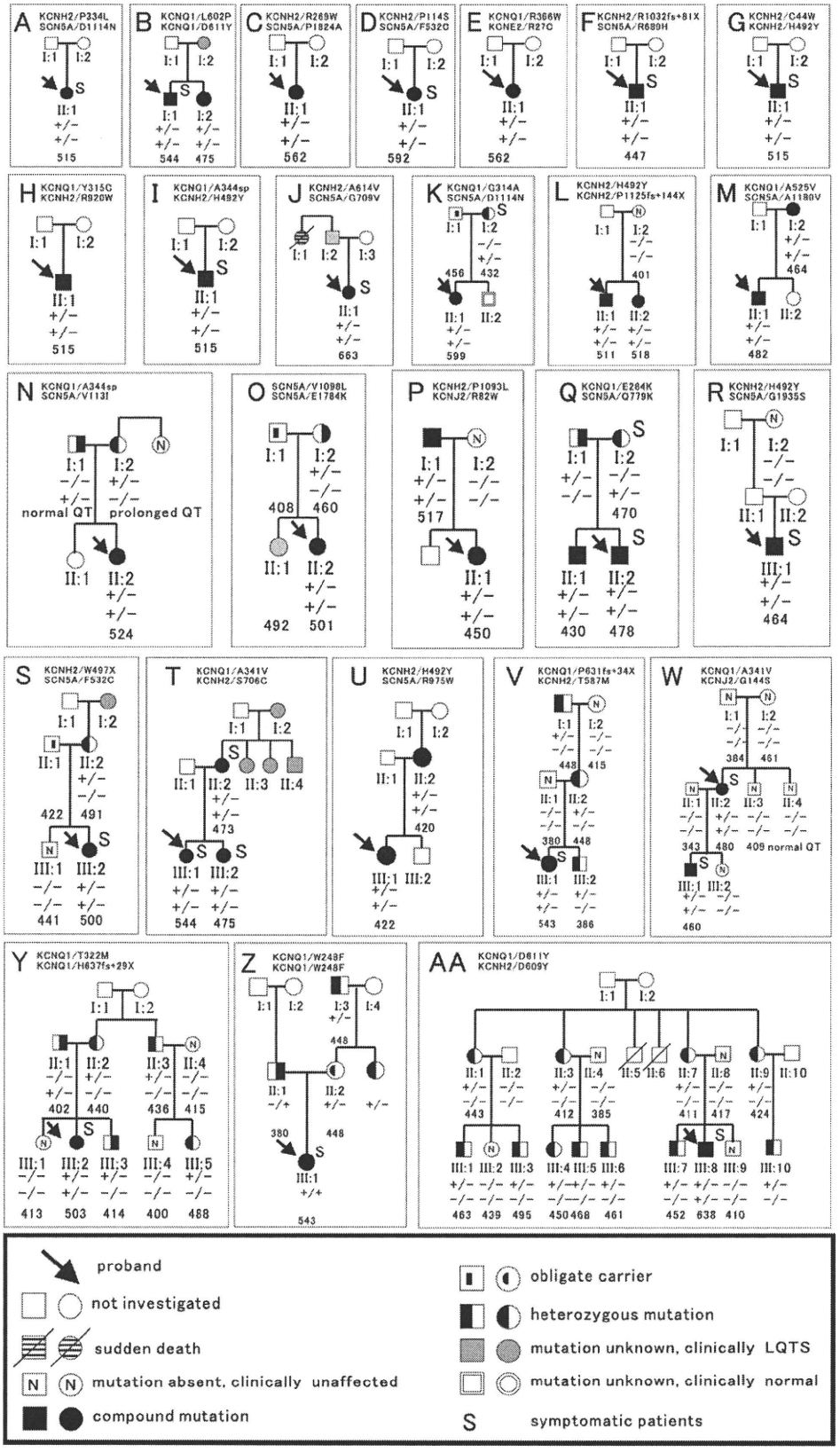

Figure 3 Pedigrees of the families associated with compound mutation probands.